A Brief Introduction to Amorphous Organic Semiconductor Film and Interface Electrical Properties

Robin A. Rice[a]

[a]University of Vermont, Burlington 05405, USA

ABSTRACT

Over the past few decades, organic semiconductors have become the subject of intense focus for their promise as highly tunable, flexible, and low-cost alternatives to the relatively mature field of inorganic semiconductors. Though the conductivity of various conjugated organic materials such as anthracene can be traced to the turn of the 20th century, it was not until the 1980s when these materials were used in organic LEDs,[1] and photovoltaics[2] that such materials, and devices thereof were considered viable.

Since then, the study of organic semiconductors (OSC) has blossomed into a field of its own, especially as OSC properties and applications extend outside that of conventional inorganic semiconductors. Yet, many challenges remain in the realm of organic electronics before they can be fully realized. Principally, a complete description of charge transport within organic materials remains in development. Nevertheless, organic semiconductors have made significant inroads in industries previously dominated by their inorganic counterparts, including xerography, LEDs, FETs, and PVs. Organic Photovoltaics (OPVs) specifically have reached efficiencies upwards of 18%[3] with potential to overtake crystalline Silicon PV (with a current efficiency record of 26%[4]) in both efficiency and cost within the next decades.

Perhaps the most interesting aspect of OSC are their unique electrical properties, which differ significantly from inorganic semiconductors. In this report, said properties will be discussed starting from a molecular perspective to inform macroscopic charge transport, band diagrams, tuning, and planar organic / organic heterojunctions. This report will conclude with a brief note on recent developments in the electrical analysis of organic semiconductor devices.

Keywords:

1. INTRODUCTION

The unique nature of OSCs originates in the organic molecule; thus it is natural to begin the discussion here. Organic semiconducting materials consist of molecular monomers. Organic semiconducting solids include molecular crystals, as well as amorphous molecular and polymeric films which represent various organizations of these molecular monomers.

Further author information: (Send correspondence to R.A.R.)
R.A.R.: E-mail: rarice@uvm.edu

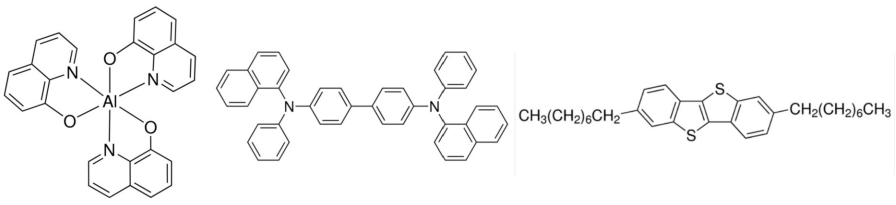

Common organic semiconducting small molecules; from left to right:N,N-Di(1-naphthyl)-N,N-diphenyl-(1,1-biphenyl)-4,4-diamine (NPB), Tris-(8-hydroxyquinoline)aluminum (AlQ3), 2,7-Dioctyl[1]benzothieno[3,2-b][1]benzothiophene (C8-BTBT)

To satisfactorily introduce all organic semiconducting solids would, and commonly does, require entire chapters. Therefore, in this report I will focus specifically on amorphous molecular solids as a common film type, typically fabricated by thermal vacuum sublimation, and with a host of interesting electrical and physical properties. A discussion of polymeric solids will simply extend from that of small molecules via their interaction in a polymer chain.

The small molecule monomers of amorphous films are hydrocarbons with selective inclusion of additional heteroatoms, with a characteristic conjugated backbone wherein adjacent sp^2 hybridized carbon atomic orbitals overlap to form bonding (σ) and antibonding (σ^*) orbitals. These hybridized bonds are generally insulating, being strong covalent bonds with empty antibonding orbitals. The remaining unhybridized p_z atomic orbitals however, overlap to produce the aforementioned characteristic bonding (π) / antibonding (π^*) frontier orbitals which are responsible for conduction.[5]

A molecule's ground state is defined as occupation of all bonding orbitals with two antiparallel electrons up to the highest unoccupied molecular orbital (HOMO), while the antibonding orbitals from the lowest unoccupied molecular orbital (LUMO), and every state of higher energy remains unoccupied. The HOMO and LUMO may be considered analogous to the valence and conduction band edge of inorganic crystalline semiconductors.

Promotion of an electron by, e.g. photoexcitation, from the HOMO to LUMO creates a neutral excited molecular state within the molecule, where an electron in an antibonding orbital leaves an empty state in the bonding orbital, constituting a hole. This neutral excited state is called an exciton. As its components are oppositely charged, they are coupled by a coulombic binding energy, called the exciton binding energy. The Bohr and critical radius of this exciton distinguish conventional semiconductors (CSC) and excitonic semiconductors (XSC) as discussed in the following section.

2. EXCITONIC SEMICONDUCTORS

An exciton in essence is a coulombically attracted positive and negative charge. As such, it may be modelled as a hydrogen atom where the exciton's Bohr radius is the orbital radius of the electron wave function from the positive hole. This electron of mass m_e, has an effective mass, m_{eff}, in a bulk with a specified dielectric constant, ϵ_r where $\epsilon = \epsilon_r\epsilon_0$, ϵ_0 being the permittivity of free space. Using the ground state Hydrogen atom Bohr radius of r_0=0.53Å, the exciton Bohr radius may be calculated:

$$r_{\mathrm{B}} = r_0\epsilon\,(m_{\mathrm{e}}/m_{\mathrm{eff}}) \tag{1}$$

The effective mass of this electron decreases with delocalization. The exciton pair may also be screened by the bulk, further lowering the binding energy between them. This is quantified by the bulk dielectric constant. Both, delocalization and increased charge screening by the bulk increase the exciton Bohr radius.

The charge carrier in question becomes free from its pair at a critical radius wherein the coulombic attraction transitions below the average thermal energy. Setting coulombic attraction equal to the thermal energy, we can solve for the critical radius:

$$E = (q^2/4\pi\epsilon\epsilon_0)(1/r_c) = k_BT \tag{2}$$

$$r_c = (q^2/4\pi\epsilon\epsilon_0 k_BT) \tag{3}$$

where E is the exciton energy, q the charge of an electron, k_B the Boltzmann constant, T the absolute temperature, and r_c the critical radius.

When $r_c > r_B$, an exciton is produced spontaneously, for example by photoexcitation. This is quantified by the parameter γ: where $\gamma > 1$ indicates XSC behavior and $\gamma < 1$ indicates CSC behavior. A γ value near 1 would not be sufficiently resolved by this model, though this is rarely the case.

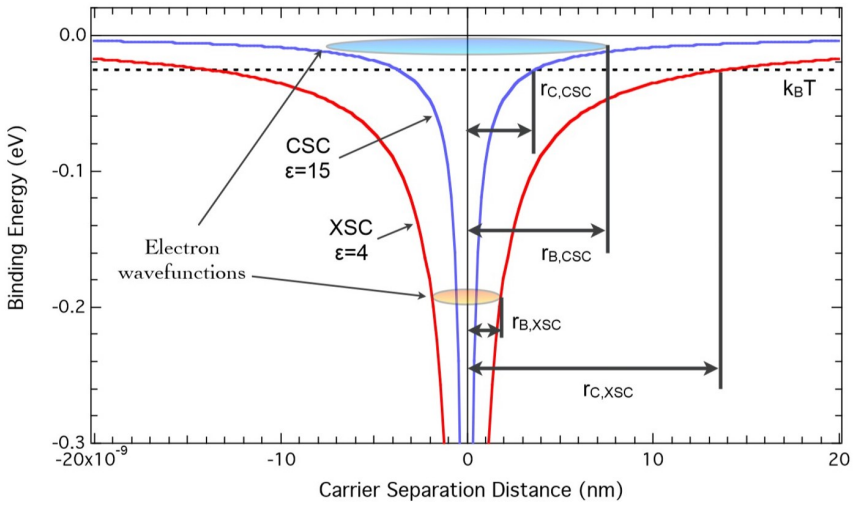

Figure 1. *The binding energies as a function of carrier separation in nm are shown for the CSC (blue) and XSC (red), note that binding energy decreases as carrier separation increases. Here the dashed horizontal line shows k_BT at some temperature. Figure reproduced by Dr. Matthew White from*[6]

In Fig.1, the binding energies as a function of carrier separation in *nm* are shown. There are two wavefunctions shown localized within the coulomb potential well for CSC (blue) and XSC (red) respectively. The thermal energy, k_BT is shown as a dotted black line. Note that as carrier separation increases, i.e. the electron wave function becomes more delocalized, the exciton binding energy decreases. If the carrier separation causes the binding energy to move below k_BT the carriers may be dissociated by the thermal energy. As expected, a larger carrier separation is required to reduce the binding energy below the thermal energy for materials of lower dielectric constants such as OSC where the carriers are less effectively screened by the bulk, resulting in an exitonic material. If the wave function fits deeper within the potential well, $\gamma > 1$ indicating excitonic behavior.

3. SMALL MOLECULE AMORPHOUS SOLIDS

As mentioned previously, small molecule amorphous films are often deposited by thermal vacuum sublimation onto the desired substrate (1 inch glass slides are common in a lab setting). In an ordered molecular or inorganic crystal, energy levels and energy level splitting would be dependent on the bulk lattice. However, in an amorphous solid, during deposition molecular energy levels shift with respect to vacuum level and environmental polarization, which if randomly varied in space, results in a gaussian (or normal) distribution of the density of states,[6] the standard deviation of which characterizes the amorphous solid's energetic disorder,[5] a broadening of the distribution corresponds to an increase in the distribution's standard deviation.

As a brief aside, some small molecules may be solution deposited as well or have their solubility increased by chemical functionalization. C8-BTBT is one example where instead of spin coating, Dr. Headrick in the physics department is developing a laminar pen-writing technique.

The technique of thermal vacuum sublimation may also be considered as relatively inefficient in material use. There are however more efficient extensions of this technique such as Organic Vapor Phase Deposition (OVPD) wherein organics are evaporated into a carrier stream of inert gas through a heated channel and directed to a cooled substrate for condensation. Another really interesting technique is supersonic molecular beam deposition wherein organics are again evaporated into a carrier gas but are then accelerated to a few eV onto the substrate allowing for the control of organics kinetic energy on film formation.[7]

3.1 Charge Hopping

Much of the basis for charge transport in disordered molecular solids lies in the Gaussian distribution model of charge hopping developed by[8] which describes the charge carrier mobility of energetically disordered materials in low field where charge carriers are thermally excited by an energy $\Delta E \sim \sigma^2/k_{\mathrm{B}}T$ from equilibrium:

Table 1. Energetic disorders of some organic semiconductors.

Material	σ [meV]	$\sigma/(k_BT)$ (at 298 K)
NPB	76	3.0
TPD	73–76	2.8–3.0
mTDATA	85–112	3.0–4.4
2TNATA	69–71	2.7–2.8
TCTA	75	2.9
P3HT	70–75	2.7–2.9
PCDTBT	130	5.1
DTP-FLU	100	3.9
Spiro-m-TTB	80	3.1
Spiro-TAD	80	3.1
Spiro-TPD	75	2.9
Spiro-MeOTAD	101	3.9

Figure 2. Energetic Disorder of various organic semiconductors. Standard deviation, σ, is listed in units of energy (meV)[9]

$$\mu = \mu_0 \exp\left[-\left(\frac{2}{3}\frac{\sigma}{k_{\mathrm{B}}T}\right)^2\right] \tag{4}$$

Energetic disorder for common organic semiconductors is listed in Fig.2. As the energetic disorder increases, being the variation in the gaussian distribution of the density of states, the energetic barrier to charge hopping increases, and mobility of the solid decreases. However, the 2/3 of Eq.(4) were extracted as an empirical fit, and the validity of this model has repeatedly been called into question, and consequently many amendments have since been proposed.[10] Note that this pseudo-classical formula for charge transport in organic semiconductors was proposed only in 1993.

Given the disordered nature of amorphous molecular films, continuous bands do not form, and charge transfer occurs between localized molecular states. This requires thermal activation of hopping where the energy required to move between localized states depends on the local molecular order, as well as relative molecular orientation and overlap of p_z orbitals in both magnitude and phase, referred to as charge transfer integral overlap[8].[10]

3.2 Doping in Amorphous Films

Inorganic semiconductors derive their utility in large part from their ability to be precisely doped such that free carriers are generated in precise concentrations and location.[6] Producing electronic states near band edges (acceptor / donor states), thereby producing free carriers in covalent solids is relatively well understood. The distortion of high energy bonds usually occurs via crystal defects including grain boundaries, or by addition of impurities of different of different valences. The same distortion is difficult in van der Waals solids where intermolecular bonds are low energy and therefore inefficient in producing free carriers, even while chemical and morphological impurity concentrations are generally far higher in van der Waals solids. Regardless, most molecular SC are considered effectively intrinsic.

Adding dopants is complicated by their significant diffusion in amorphous films. Dopants such as O_2, Br, I in a van der Waals solid with a weak lattice will significantly diffuse over time. Even larger dopants like $F4{-}TCNQ$ still diffuse too quickly to support a stable p-n junction, which is ultimately destroyed by recombination of dopants and carriers. Rather, doping in molecular OSC is usually chemically or morphologically adventitious which can preferentially trap specific carriers, resulting in an “n-type” or “p-type” material.

As will be discussed, the exact nature of these trap sites, and or disorder as a whole in disordered semiconductors, remains obscure and so many materials are not specifically designed to be preferential hole or electron conductors but are rather known as having or not having preferential conduction. MoO3 for example is a material very commonly used as a hole injection layer.[11]

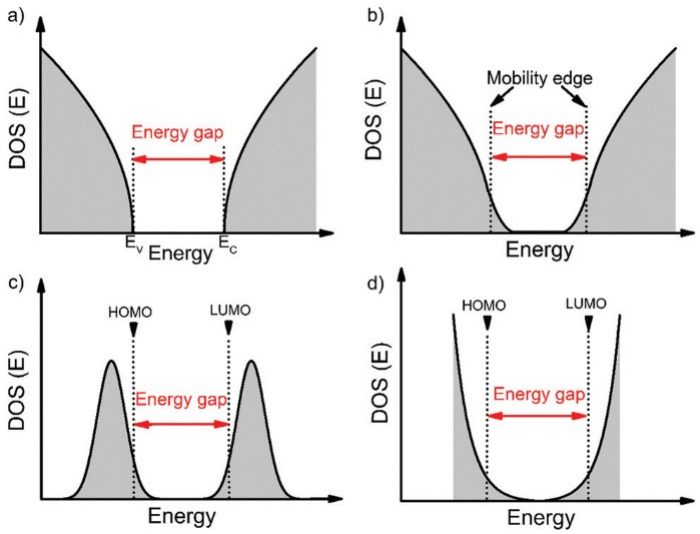

Figure 3. The density of states (DOS) for various materials; a) crystalline Silicon, b) amorphous silicon, c) d) amorphous film of small molecule and / or polymeric organic semiconductors. The Energy gap in c-Si is clear as there are very few trap sites, while in disordered solids b)c)d) the mobility edge is used to determine the bandgap. c) shows a gaussian DOS with tail states above and below the HOMO and LUMO respectively. d) shows an abbreviation of the guassian distribution focusing on the tail states within the bandgap. Carriers which are thermally activated to tail states within the bandgap contribute to conduction, while those below and above the HOMO and LUMO are localized.[?]

3.3 Trap States in Disordered Films

Energetic disorder within amorphous organic semiconductors can create shallow trap states within the bandgap either near the HOMO or LUMO causing preferential conduction of charge carriers and subsequent 'n-type' or 'p-type' behavior. These states near the band edges are caused by pushing the tail states of the localized DOS in OSC of the HOMO or LUMO into the band gap. These tail states then act as shallow trap states.

As will be shown, whether and to what degree a material is an acceptor or donor may be accomplished by design of HOMO and LUMO energy levels, which may be tuned by chemical functionalization. In this way, the energy states and thus the core of charge transport properties of organic semiconductors is opened to the massive synthetic power of organic chemistry.

The DOS describes the energetic distribution of electronic states within energy bands, specifically, the number of states per energy per unit volume. A covalent solid such as c-Si will have a parabolic DOS (Fig.3a) with well-defined band edges. As the localization of these states increases, extended states create tails in the band gap, (Fig.3b for amorphous Si) which are modelled exponentially. This is seen more clearly in disordered semiconductors with energy states that take a fully gaussian distribution, which itself can be abbreviated as an exponential distribution (seen in Fig.3c and Fig.3d for disordered semiconductors). When tail states as signatures of disorder are present, there is no longer a clear band gap and so a mobility edge is used denoting the transition from extended (delocalized) to localized states – with an accompanying change in charge carrier mobility. You can see this schematically in Fig. 3b as the inflection point of the DOS.

As we shall see, these band tail states are critical to the charge transport properties of disordered materials. However, even though the general form of tail states is accepted a quantitative description of the tail state energy spectrum is unknown for most all disordered materials. Without a detailed description of these band states, it is extremely difficult to develop a complete quantitative theory of charge transport in disordered materials, and could be considered one of the principle challenges in the field of disordered organic semiconductors.[12]

For example, slow thermodynamic relaxation of disordered materials toward equilibrium which varies by deposition technique, temperature, environmental polarization, etc. can significantly complicate charge transport, especially at low temperatures where electron tunneling between localized states occurs, which is extremely sensitive to the spatial and energetic distance between localized states.[12]

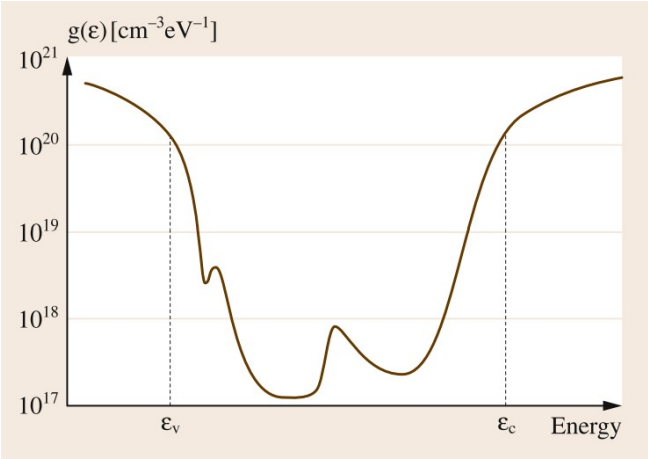

Figure 4. The DOS of a non-crystalline semiconductor. E_v and E_c are the mobility edges corresponding to valence and conduction edges, while peaks within the bandgap are likely due to high concentration defect states[12]

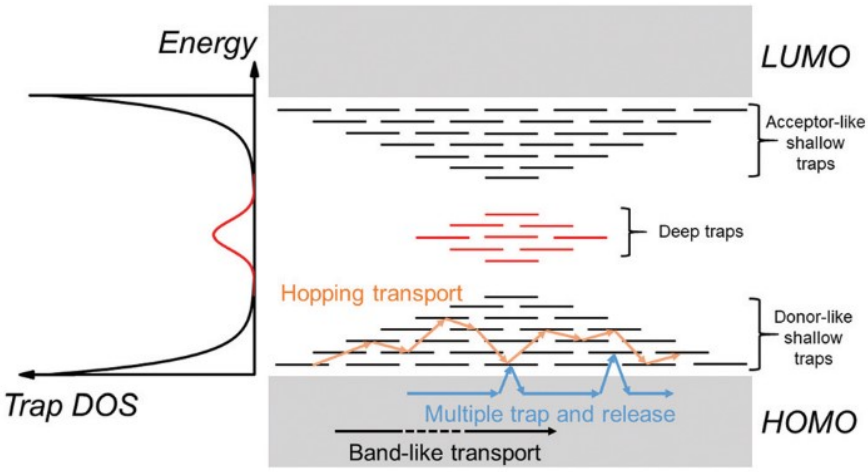

Figure 5. Gaussian distribution of deep trap states (red) in the center of the band gap and exponential distributions of disorder induced tail states (black) which extend into the band gap as shallow traps[13]

A gaussian distribution of deep trap states (red) in the center of the band gap is shown in Fig.5 and exponential distributions of disorder induced tail states (black) which extend into the band gap as shallow traps. These exponential distributions simply model the extended tail states of localized gaussian DOS distributions of the HOMO and LUMO. Once these tail states are extended into the band gap, the tail states are what inform conduction and so the gaussian is often abbreviated by an exponential.

Importantly, if the trap depth being the energetic distance of trap states from the band edge is shallow, as in localized tail states, they may behave as acceptor or donor-like traps. Shallow traps near above the valence mobility edge, near the HOMO, can behave as donor-like shallow traps. These traps can capture or restrain charge carriers until they are released to the band by external stimulus e.g. electric field, thermal energy, or photoexcitation. The blue arrows show the multiple trap and release (MTR) model where charges moving via delocalized band states are trapped in localized shallow bandgap states and again, while high trap densities allow trapped (localized) charge carriers to move between localized trap states via thermally activated hopping or tunneling, known as charge hopping.[?]

Most small molecule amorphous OSC films have a low transfer integral and therefore high energetic barriers for charge hopping between molecules, resulting in low mobility solids and space charge limited current. In fact, most OSC charge carrier mobilities are below 10 cm^2/Vs while mobilities in crystalline silicon and graphene range in the order of $1e3$ $\mathrm{cm}^2V^{-1}s^1$ and $1e6$ $\mathrm{cm}^2V^{-1}s^1$, many magnitudes higher[?]). Consequently, these solids do not have the long-range order typical of ISCs and molecular crystals.

Interestingly, as these solids lack long range order, they also lack grain boundaries and therefore exhibit notable mechanical properties including the ability to function if deposited on a flexible substrate. This enables organic electronics to be applied in wearable electronics, bioelectronics, flexible displays and solar panels.

4. ORGANIC-ORGANIC HETEROJUNCTIONS

Heterojunctions denote the interface of any two solid state materials, being crystalline or amorphous metals, insulators, or semiconductors. Organic heterojunctions likewise denote the interface of two organic semiconductors. These are functionally distinct from inorganic heterojunctions, as will be discussed in this section.

Organic semiconductors do not have a large concentration of free carriers and so little band bending occurs for many O/O heterojunctions in which case the junctions may be described by the Shockley-Mott model of flat energy levels, and aligned junction vacuum levels. This is seen for example in NPB/AlQ3 junctions. There are however strong electron donor / acceptor junctions with significant band bending and majority carrier accumulation type junction and a highly conductive space charge region being full of mobile majority carriers. This is seen in CuPc/F16CuPc and BP2T/F16CuPc junctions.

However, it should be emphasized that the fundamental theory of organic-organic heterojunctions remains in flux. Here we will explore the recent series of charge transport investigations of a simple amorphous planar heterojunction OLED device.

4.1 OLED Heterojunction

Beginning with the work of,[15] an impedance spectroscopy capacitance-voltage investigation was presented which detailed hole accumulation at the organic TPD/AlQ3 interface before sufficient applied bias allowed the carriers to diffuse across the TPD/AlQ3 HOMO barrier and radiatively recombine with electrons in AlQ3 layer.

This is described succinctly in a C-V plot with a corresponding series of band diagrams wherein once applied bias $V_0 = V_t$ reaches a flatband voltage for the TPD layer holes begin to diffuse from the ITO anode to the TPD/AlQ3 HOMO barrier where they accumulate. Further positive applied bias until $V_0 = V_{bi}$ reaches the built in voltage due to the work function difference of the electrodes when electrons begin to likewise diffuse from the cathode (here Calcium) to the interface. As described by Nowy, once a characteristic voltage is reached the accumulated holes overcome the HOMO organics interface barrier and radiatively recombine with the electrons in the AlQ3.

This is seen in parallel in the C-V plot wherein the device begins with a constant geometric capacitance at low voltage, begins to accumulate holes as positive charge once $V_0 = V_t$, until maximum capacitance at $V_0 = V_{bi}$, followed by a sudden decrease in capacitance by recombination charge annihilation.

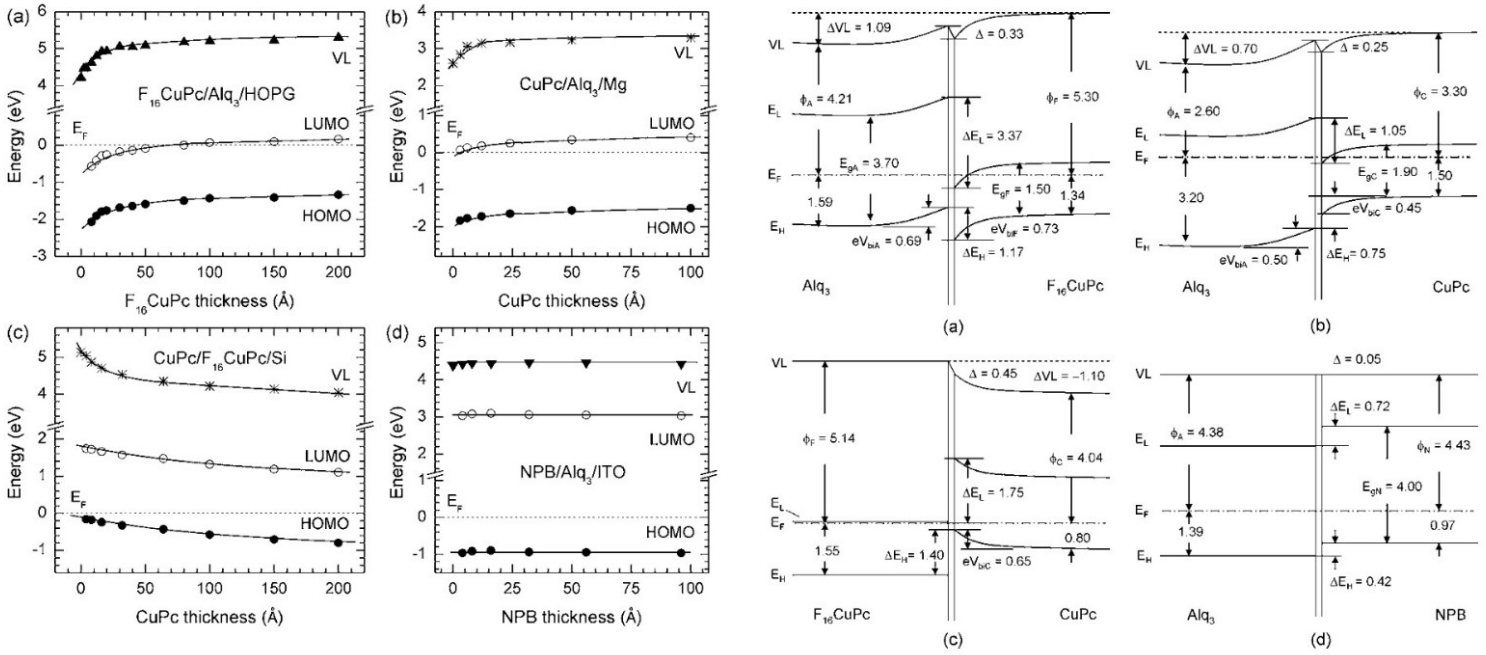

Figure 6. left: HOMO, LUMO, and vacuum level shifts for a) F16CuPc in F16CuPc/Alq3, b) CuPc in CuPc/Alq3, c) CuPc in CuPc/F16CuPc, and d) NPB in NPB/Alq3 calculated via UPS measurements, where zero energy represents the Fermi level, as indicated. right: Energy level diagrams for the interfaces detailed in the left set of figures, a) F16CuPc/Alq3 hetero- junction on highly oriented pyro- lytic graphite (HOPG), b) CuPc/Alq3 heterojunction on Mg, c) CuPc/F16CuPc heterojunction on Si, and d) NPB/Alq3 heterojunction on ITO, shown in eV. The substrates work functions of HOPG, Mg, Si, and ITO are estimated to be 4.43, 3.75, 3.95, and 4.95 eV, respectively.[14]

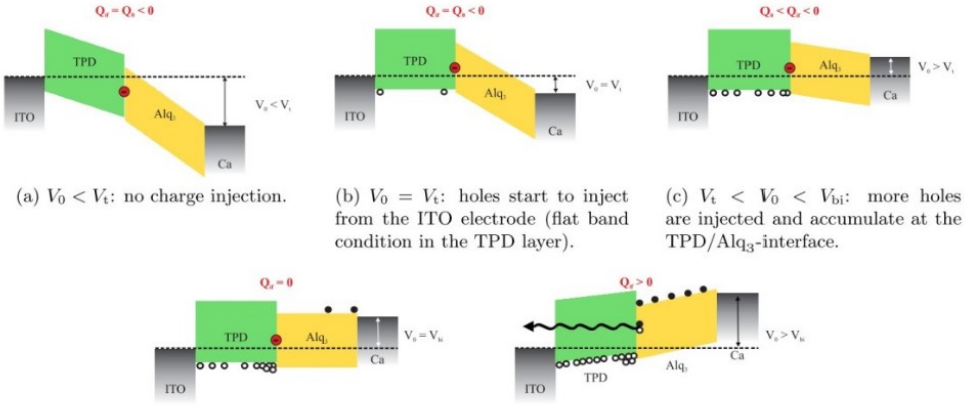

(a) $V_0 < V_t$: no charge injection.

(b) $V_0 = V_t$: holes start to inject from the ITO electrode (flat band condition in the TPD layer).

(c) $V_t < V_0 < V_{bi}$: more holes are injected and accumulate at the TPD/Alq_3-interface.

(d) $V_0 = V_{bi}$: electrons start to inject from the Ca electrode (flat band condition in the Alq_3 layer).

(e) $V_0 > V_{bi}$: more electrons are injected into the OLED and recombine with the holes under emission of light.

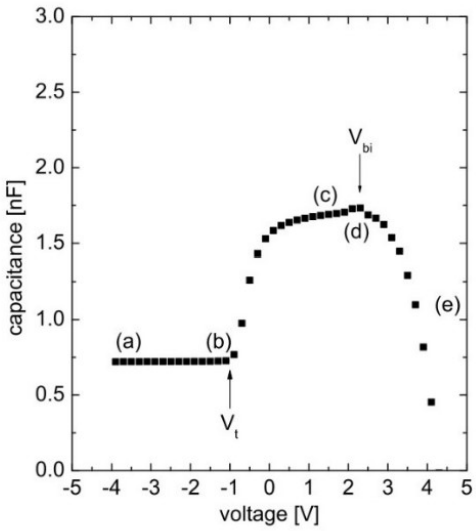

Figure 7. left: OLED (ITO/TPD/AlQ3/Ca) band diagrams for various applied voltages; right: capacitance-voltage plot for the same device with corresponding applied voltage indications.[15]

Takahasi et al.[16] then contends that these accumulation charges are actually due to interface states which are a result of energetic disorder due to the amorphous vacuum evaporated deposition nature of the interface, using a very similar device structure of ITO/NPB/AlQ3/LiF/Al. This process is referred to as Activated Localized Carrier Source (ACLS)

Given the vacuum deposition of layers, traps near the HOMO form which are shallow enough to be thermally activated at room temperature, which at low applied bias, when the internal electric field points from NPB/AlQ3 to ITO/NPB, from the organics interface to ITO, and since the majority of the NPB layer is insulating (i.e. no charge transport), a buildup of charges occurs near the organics interface. Once NPB flatband is reached, the carriers (holes) diffuse in the NPB region near the organics interface and make that region conductive. Once the built in voltage is overcome by the applied voltage, the internal electric field flips to direct from anode (ITO) to cathode (Al/LiF), pushing the accumulated holes to the AlQ3 barrier at the organics interface. Once device flatband is reached, electrons diffuse into the AlQ3 from the cathode (LiF/Al). At a characteristic positive applied bias, the holes will overflow / overcome the NPB/AlQ3 HOMO barrier and diffuse into the AlQ3 where they will recombine in the AlQ3 with the cathode injected electrons.

This is shown diagrammatically in,[15] with the caveat that that diagram shows holes being sourced by injection rather than thermally activated localized states within NPB.

The following year, Takahashi et al. extended their previous investigation builds on both accumulation and ACLS models, expressed in a band diagram showing a voltage difference across the contacts progression from insulation, accumulation of charge at interface barriers, finally the applied voltage fully counters the built in voltage of work function difference of the contacts allowing the internal electric fields within NPB and AlQ3 to direct from anode to cathode allowing for carrier flow to be contact injection limited or bulk charge hopping limited. As an OLED, holes and electrons recombine in the AlQ3 emission layer.

Importantly, the accumulation of holes – which at sufficient positive bias surmount the interface barrier – is supplied by interface states *rather* than by the electrode which maintains thermal equilibrium of the interface states. In this way, heterojunctions may be used to voltage control carrier transport in organic semiconductors.

This in contrast to Schottky barriers of inorganic semiconductor/metal heterojunctions wherein band bending due to fermi level alignment creates a depletion zone from a neutral conducting state of the semiconductor. Organics, rather, evolve from a neutral insulating state into a conducting one. This point emphasizes that Tang and van Slyke who invented the first functional organic diode were not merely discovering a replacement for Silicon, but establishing an entirely distinct branch of semiconductor device physics.[17]

5. NONLINEAR IMPEDANCE SPECTROSCOPY (NLIS)

Ultimately my research focuses on developing a novel nonlinear extension of Impedance Spectroscopy, and using organic electronics as a benchmark case study wherein results from the nonlinear analysis may be compared with the extensive literature on the Impedance Spectroscopy of the same or very similar device structures and material properties.

These essence of the NLIS technique lies in being able to experimentally measure the derivatives of the dominant current-voltage transfer function at any given voltage across a wide frequency range (typically 1Hz – 1MHz in our experiments).[18] Given Impedance Spectroscopy functions at the low end of that frequency spectra, results from the nonlinear to (linear) impedance spectroscopy investigations may be bridged via low frequency values, such that the validity of previously unstudied higher frequency values may be validated.

While the theory of amorphous small molecule organic / organic (O/O) heterojunctions is very much still being elucidated, the general form of the Shockley diode equation may be used here. Though many texts are devoted to a physical basis of the diode equation for O/O heterojunctions, as will be shown, the technique presented here will use the spacing between derivatives of the diode transfer function to extract the diode ideality constant of a device or active layer, bypassing the need to ascribe physical interpretation to the saturation, diffusion, or drift currents of a device beyond their general form of which a general consensus exists. Derivations of the physical interpretation of the diode behavior of O/O heterojunctions,[19] energy level alignment of O/O heterojunctions,[14] and electrical properties of O/O heterojunctions[20] may be found in literature.

6. CONCLUSION

Organic semiconductor materials and devices are an incredibly exciting class electronics, not only for their ability to challenge the dominance of inorganic semiconductors, but for their distinct physical and electrical properties. By pairing the massive synthetic and commercial power of organic chemistry, organic semiconductors hold the potential to usher a new era of low-cost, sustainably sourced, flexible, and tunable solar, and displays.

ACKNOWLEDGMENTS

I would like to thank my advisor Dr. Matthew White for guiding me from the ground up over my graduate career, and all the professors I have had the pleasure of taking a course with.

REFERENCES

[1] C. W. Tang and S. A. Vanslyke, "Organic electroluminescent diodes," *Applied Physics Letters*, vol. 51, no. 12, pp. 913–915, 1987.

[2] C. W. Tang, "Two-layer organic photovoltaic cell," *Applied Physics Letters*, vol. 48, no. 2, pp. 183–185, 1986.

[3] M. Zhang, L. Zhu, G. Zhou, T. Hao, C. Qiu, Z. Zhao, Q. Hu, B. W. Larson, H. Zhu, Z. Ma, Z. Tang, W. Feng, Y. Zhang, T. P. Russell, and F. Liu, "Single-layered organic photovoltaics with double cascading charge transport pathways: 18% efficiencies," *Nature Communications*, vol. 12, no. 1, pp. 1–10, 2021. [Online]. Available: http://dx.doi.org/10.1038/s41467-020-20580-8

[4] NREL, "Best Research-Cell Efficiency Chart.pdf," p. 1, 2019. [Online]. Available: https://www.nrel.gov/pv/assets/pdfs/best-research-cell-efficiencies.20190802.pdf

[5] H. Bassler and A. Kohler, "Charge Transport in Organic Semiconductors," *Springer*, vol. 310, no. October 2011, pp. 1–26, 2011.

[6] B. A. Gregg, S. G. Chen, and R. A. Cormier, "Coulomb forces and doping in organic semiconductors," *Chemistry of Materials*, vol. 16, no. 23, pp. 4586–4599, 2004.

[7] N. Koch, "Organic electronic devices and their functional interfaces," *ChemPhysChem*, vol. 8, no. 10, pp. 1438–1455, 2007.

[8] H. Bässler, "Charge Transport in Disordered Organic Photoconductors a Monte Carlo Simulation Study," *Physica Status Solidi (B)*, vol. 175, no. 1, pp. 15–56, 1993.

[9] H. Li, C. Li, L. Duan, and Y. Qiu, "Charge transport in amorphous organic semiconductors: Effects of disorder, carrier density, traps, and scatters," *Israel Journal of Chemistry*, vol. 54, no. 7, pp. 918–926, 2014.

[10] M. Wojcik, I. Zawieja, and K. Seki, "Charge Transport in Disordered Organic Solids: Refining the Bässler Equation with High-Precision Simulation Results," *Journal of Physical Chemistry C*, vol. 124, no. 33, pp. 17 879–17 888, 2020.

[11] M. Kröger, S. Hamwi, J. Meyer, T. Riedl, W. Kowalsky, and A. Kahn, "Role of the deep-lying electronic states of MoO3 in the enhancement of hole-injection in organic thin films," *Applied Physics Letters*, vol. 95, no. 12, 2009.

[12] S. Baranovskii and O. Rubel, "Charge transport in disordered materials," *Springer Handbooks*, p. 1, 2017.

[13] H. F. Haneef, A. M. Zeidell, and O. D. Jurchescu, "Charge carrier traps in organic semiconductors: A review on the underlying physics and impact on electronic devices," *Journal of Materials Chemistry C*, vol. 8, no. 3, pp. 759–787, 2020.

[14] J. X. Tang, C. S. Lee, and S. T. Lee, "Electronic structures of organic/organic heterojunctions: From vacuum level alignment to Fermi level pinning," *Journal of Applied Physics*, vol. 101, no. 6, pp. 1–5, 2007.

[15] S. Nowy, W. Ren, J. Wagner, J. A. Weber, and W. Brütting, "Impedance spectroscopy of organic hetero-layer OLEDs as a probe for charge carrier injection and device degradation," *Organic Light Emitting Materials and Devices XIII*, vol. 7415, p. 74150G, 2009.

[16] J. ichi Takahashi and H. Naito, "Visualization of the carrier transport dynamics in layered Organic Light Emitting Diodes by Modulus spectroscopy," *Organic Electronics*, vol. 61, no. April, pp. 10–17, 2018. [Online]. Available: https://doi.org/10.1016/j.orgel.2018.06.056

[17] J. I. Takahashi, "Negative impedance of organic light emitting diodes in AC electrical response," *Journal of Applied Physics*, vol. 125, no. 24, 2019.

[18] A. Larsen, E. Dahal, J. Paluba, K. Cianciulli, B. Isenhart, M. Arnold, B. Du, Y. Jiang, and M. S. White, "Nonlinear impedance spectroscopy of organic MIS capacitors and planar heterojunction diodes," *Organic Electronics*, vol. 62, no. July, pp. 660–666, 2018. [Online]. Available: https://doi.org/10.1016/j.orgel.2018.07.003

[19] N. C. Giebink, G. P. Wiederrecht, M. R. Wasielewski, and S. R. Forrest, "Ideal diode equation for organic heterojunctions. I. Derivation and application," *Physical Review B*, vol. 82, no. 15, pp. 1–12, 2010.

[20] D. Ma, *Organic semiconductor heterojunction and its application in organic light-emitting diodes (Conference Presentation)*, 2016.